Table des Matières

Présentation

Ce travail a été réalisé dans le cadre d'une thèse en cotutelle entre l'Université Joseph Fourier (Grenoble,France) et l'Universitat Autònoma de Barcelona (Espagne). Cette recherche a été faite principalement dans le Laboratoire Louis Néel (CNRS-Grenoble) et l'Institut de Ciència de Materials de Barcelona (CSIC). Cependant de nombreuses expériences ont requis l'utilisation de grands instruments comme ceux de l'Institut Laue-Langevin (ILL-France), European Synchrotron Radiation Facility (ESRF-France), ISIS (Royaume Uni), et du Service National de Champs Magnétiques Pulsés (SNCMP-Toulouse).

L'étude des manganites à valence mixte ($RE^{+3}_{1-x}B^{+2}_{x}\ MnO_3$) a commencé dans les années cinquante [1-3]. Néanmoins l'intérêt pour ces matériaux a été renouvelé dans les années quatre vingt dix [4] dû à la potentielle utilisation technologique de la magnétorésistance colossale présentée par certaines manganites ferromagnétiques ($x\approx0.3$) et, d'un point de vue fondamental, à l'intérêt de l'étude de leur caractère demi-métallique et de la compréhension des interactions complexes dans ces oxydes fortement corrélés. En plus, récemment, l'existence d'une forte magnétorésistance et d'un faible ferromagnétisme a été découverte dans une région étroite du diagramme de phase dans les manganites fortement dopées en trous [5] et son origine a été dévoilé dans cette thèse. Si l'utilisation de cette famille de matériaux dans les applications possède plusieurs inconvénients (faible température de Curie, faible sensibilité en champ et résistivité élevée), l'importance des manganites est plus claire par leur caractère de système modèle pour plusieurs études fondamentales en raison du fort couplage entre les degrés de liberté magnétique, orbital, cristallographique et électronique. La compréhension complète de la variété d'états fondamentaux, propriétés et transitions dans ces composés (ferromagnétisme-FM, antiferromagnétisme-AFM, ordre orbital-OO, ordre des charges-CO, ségrégation électronique, demi-métallicité,, effet isotopique, transition métal/isolant-M/I) reste encore un défi pour les physiciens de l'état solide.

Dans ce travail, nous avons étudié plusieurs phénomènes avec une approche fondamentalement différente. Pour cette raison, nous avons divisé ce manuscrit en deux parties. Chaque partie est auto consistante, à l'exception des chapitres 1 et 2 qui sont des chapitres introductifs aux manganites et à la magnétorésistance respectivement.

Dans la **Partie I,** nous présentons l'étude de la croissance des couches minces des manganites sur des substrats monocristallins. Ce travail se focalise sur le composé ferromagnétique à base de lanthane avec un dopage optimal en calcium de $x=1/3$, qui a un caractère demi-métallique à l'état ferromagnétique. La compréhension des phénomènes qui contrôlent les propriétés de ce matériau, ainsi que l'effet de la contrainte sont essentielles pour l'utilisation technologique de sa bande de conduction fortement polarisée en spin.

Deux thèmes ont été étudiés dans cette partie. Dans le chapitre 3 nous aborderons le transport de spin à travers les interfaces dans des couches minces de $La_{2/3}Ca_{1/3}MnO_3$. L'intérêt principal a été de comprendre les effets d'existence de joints de grain et de la Magnétorésistance de Poudres (PMR) dans ces composés. Pour cette raison, nous avons créé des systèmes artificiels modèles, comme des couches polycristallines obtenues sur des substrats monocristallins non accordés en paramètre de maille, des couches déposées sur des substrats gravés ou bien des couches texturées avec des défauts cristallographiques contrôlés, qui nous ont permis trouver le rôle des interfaces dans le transport dépendant du spin. Des mesures sans précédent de magnétorésistance et d'effet Kerr à champs magnétiques forts (30T) et des mesures de I(V) à des températures de l'ordre de quelques dizaines de mK sur des systèmes avec et sans interfaces sont présentées et discutées.

Dans le chapitre 4, nous avons étudié le rôle de la contrainte épitaxiale dans la réponse magnétorésistive dans des couches de $La_{2/3}Ca_{1/3}MnO_3$ sur $SrTiO_3$ (001). Dans ce système, la modification des propriétés magnétiques et de transport a été discutée et liée à la déformation structurale induite par la croissance épitaxiale.

La **Partie II** est dédiée à l'étude des différents types de phénomènes de ségrégation électronique et macroscopique dans des composés massifs fortement dopés en trous ($A^{+3}_{1-x}B^{+2}_{x}MnO_3$ x [0.5-1]). Tout d'abord, nous présentons l'étude de la transition métal/isolant, structurale et magnétique induite par la redistribution électronique dans $Pr_{1/2}Sr_{1/2}MnO_3$ (chapitre 6). L'effet du replacement de Sr^{2+} par Ca^{2+}sur l'ordre orbital et des charges ainsi que la ségrégation de phase électronique et l'hétérogénéité magnétique dans le composé $Pr_{2/3}Ca_{1/3}MnO_3$ sont présentées dans le chapitre 7, où nous montrons la distribution spatiale des hétérogénéités magnétiques à partir des résultats expérimentaux de diffraction de neutrons et des expériences de relaxation de muons.

Finalement, dans le chapitre 8, différents types de coexistence de phases ont été analysés dans la zone riche en trous des composés $Bi_{1-x}Ca_xMnO_3$. La modulation structurale du composé x=1/2 a été déterminée sans ambiguïté grâce à la large différence des paramètres de maille. Une étude comparative avec le composé à base de lanthane a été faite, ce qui a permis de déterminer l'effet du Bi^{+3} $6s^2$ "lone pair". De plus, la coexistence d'un ordre orbital quasi-dégénéré a été suivie dans le composé x=2/3 grâce à des mesures de diffraction de rayons X et de neutrons de haute résolution. Enfin, les composés avec un dopage plus élevé en trous (x=0.85 et x=0.875) qui présentent des valeurs élevées de magnétorésistance et un faible ferromagnétisme, ont été étudiés. La séparation de phase macroscopique a été observée et l'origine de la magnétorésistance a été interprétée à partir des résultats de diffraction à haute résolution.

Les deux thèmes de recherche développés dans cette thèse ont été présentés séparément dans ce manuscrit comme **Partie I** et **Partie II**. Ils doivent être considérés comme un choix personnel, un désir d'acquisition d'une plus large connaissance des vastes domaines de la Physique de l'état solide et à la compréhension des phénomènes étroitement liés aux systèmes à électrons fortement corrélés.

Presentation

This thesis has been carried out in the framework of a co-thesis between the Université Joseph Fourier (Grenoble-France) and the Universitat Autònoma de Barcelona (Spain). The research has been undertaken mainly at the Laboratoire Louis Néel (CNRS-Grenoble) and Institut de Ciència de Materials de Barcelona (CSIC). However, several experimental techniques also required the use of large European Facilities as those at Institut Laue-Langevin (ILL-France), European Synchrotron Radiation Facility (ESRF-France), ISIS (United Kingdom) and at the french Service National de Champs Magnétiques Pulsés (SNCMP-Toulouse).

Mixed valence manganites ($A^{+3}_{1-x}B^{+2}_{x}\,MnO_3$) were firstly studied in the fifties [1-3]. However a renewed interest appeared in the nineties [4] due to the potential technological use of the colossal magnetoresistance that certain ferromagnetic manganites ($x\approx0.3$) exhibit and, from the fundamental point of view, due to the interest of the study of their half metallic character and the of comprehension of the complex interactions in these strongly correlated oxides. In addition, it has recently been discovered the existence of large magnetoresistance and weak ferromagnetism in a narrow range of the phase diagram in some heavily hole doped manganites [5] and its origin is elucidated in this thesis. Even if the use of this family of compounds in applications has several disadvantages (low Curie temperature, low sensitivity to the applied field, large resistivity..), the importance of manganites is more clear as a model system for several fundamental studies due to the strong coupling between the magnetic, orbital, electronic and crystallographic degrees of freedom. Deep understanding the variety of ground states, properties and transitions in these compounds (ferromagnetism-FM, antiferromagnetism-AFM, charge ordering-CO, orbital ordering-OO, isotopic effects, metal/ insulator-M/I transitions..) is still a challenge for solid state physicists.

In the present work, we have studied different phenomena associated to manganite compounds with an approach fundamentally different. For that reason, we have divided the present manuscript in two parts. Each part is self-consistent except chapter 1 and chapter 2, which are introductory chapters to manganites compounds, and to magnetoresistance respectively.

In **Part I** we present the study of the growth of manganite based thin films on single crystalline substrates. This work focuses on ferromagnetic lanthanum based manganites with an optimum Ca doping of x=1/3, which exhibit Colossal Magnetoresistance at the metal/insulator transition temperature. Such compounds are half-metallic in the ferromagnetic state, so the understanding of possible tuning mechanisms, as well as epitaxial strain induced effects are essential for the technological use of their highly polarised conduction band.

Two different remarkable issues have been studied in this part. In chapter 3 we have studied the spin transport through the interfaces in $La_{2/3}Ca_{1/3}MnO_3$ thin films. The main interest is to get more insight

in the understanding of the granular effects and the Powder Magnetoresistance in these compounds. For that reason, several artificially created model systems have been used as polycrystalline films obtained on non lattice matched single substrates, thin films grown on scratched single crystalline substrates and textured films with controlled crystallographic defects which have allowed us to get a better description of the effect of interfaces on the spin transport. Measurements of magnetoresistance and Kerr effect manganites under high magnetic fields (30T) as well as I(V) measurements at temperatures of the order of some tenths of mK on systems with and without interfaces are shown and interpreted.

In chapter 4, we present the study the role of epitaxial strain on the magnetoresistive response of $La_{2/3}Ca_{1/3}MnO_3$ (001) films grown on $SrTiO_3$. The modification of the magnetic and transport properties is been discussed and related to the structural deformation induced by the epitaxial growth.

Part II is mainly devoted to the study of different types of phase separation phenomena on bulk compounds in the highly hole doped manganites ($A^{+3}_{1-x}B^{+2}_{x}$ MnO_3 x [0.5-1]). Firstly, we present the study of the metal/insulator, structural and magnetic transition induced by electronic re-distribution in $Pr_{1/2}Sr_{1/2}MnO_3$ (chapter 6). The effect of the full substitution of Sr^{2+} by Ca^{2+} on the orbital and charge ordering is presented in chapter 7, as well as the electronic phase segregation, magnetic inhomogeneity and disorder in $Pr_{2/3}Ca_{1/3}MnO_3$ bulk samples. In the light of neutron powder diffraction data and Zero-Field Muon Spin Relaxation measurements, the spatial distribution of the magnetic inhomogeneities has been determined.

Finally, in chapter 8 several types of phase coexistence have been analysed in the heavily hole doped region of $Bi_{1-x}Ca_xMnO_3$. The structural modulation for the x=1/2 compound has been unambiguously determined thanks to the large difference in cell parameters. A comparative study has been performed with the parent compound of lanthanum based manganite which allowed determining the effect of Bi^{+3} $6s^2$ lone pair. The coexistence of quasi-degenerate orbital ordering has been followed on powder samples of compositions x=2/3 thanks to high resolution powder diffraction data. Finally, the compounds with larger hole doping level, x=0.85 and x=0.875, presenting large values of magnetoresistance and weak ferromagnetism have been studied and the macroscopic phase separation and magnetoresistance have been interpreted on the basis of joint high resolution synchrotron and neutron powder diffraction experiments.

The two research subjects carried out during this thesis are separated in this manuscript as **Part I** and **Part II**. They should be considered as a personal choice, a wish towards the acquisition larger knowledge in broad fields of the solid state physics and the understanding of striking phenomena highly related to the strongly correlated electronic systems.

Partie I

Introduction à la Partie I

L'utilisation des propriétés de beaucoup de matériaux fonctionnels nécessite souvent leur préparation en couches minces. Les propriétés physiques d'un matériau, comme l'anisotropie, les interactions magnétiques ainsi que les propriétés structurales et électriques, peuvent être fortement modifiées, quand il est sous forme de couche mince, à cause de la contrainte induite par le substrat ou bien par le changement du rapport surface/volume .

Ce travail est le premier travail dédié à la croissance des couches minces de manganites au Laboratoire Louis Néel. L'objectif a été l'étude et l'optimisation de la croissance des couches de manganite déposées sur des substrats monocristallins, ainsi que l'étude de leurs propriétés magnétiques et de transport, avec une attention spéciale portée au transport dépendant du spin. Ces objectifs demandaient le développement d'une nouvelle chambre d'ablation laser, spécialement adaptée à la croissance des oxydes (Appendix A:). Pour cette raison, j'ai consacré une partie considérable de mes efforts à la conception et à la mise en fonctionnement de cette nouvelle chambre d'ablation laser.

Dans la **Partie I,** nous donnons une description générale des perovskites de manganèse. Leur structure cristallographique ainsi que leurs propriétés magnétiques et électriques sont importantes pour la compréhension du présent travail de recherche (chapitre 1). Dans un deuxième temps, nous présentons une brève introduction aux bases du transport électrique dans les matériaux ferromagnétiques, ainsi qu'au transport dépendant du spin (magnétorésistance, MR) et leur origine (Chapitre 2).

L'étude de la croissance de $La_{2/3}Ca_{1/3}MnO_3$ sur des substrats non accordés en paramètre cristallin ainsi que l'étude des effets de granularité associés à la magnétorésistance des poudres (PM) ont été effectuées sur des couches polycristallines et sur des joints de grains induits par des nouvelles méthodes non-conventionnelles (Chapitre 3). L'effet de la contrainte induite par la croissance épitaxiale sur des substrats accordés en paramètre cristallin (propriétés magnétiques, de transport et cristallographiques) est discuté et analysé (Chapitre4).

L'originalité de ce travail réside dans sur le fait que, pendant que de nombreux efforts ont été dédiés à l'étude des manganites présentant des valeurs élevées de la MR à température ambiante et des systèmes hétérostructurés (jonctions tunnel), peu avaient été menés sur le transport dépendant du spin à travers des interfaces des manganites.

La compréhension du transport dépendant du spin à travers des joints de grains ou dû à la contrainte dans des couches de manganites est fondamentale avant de développer des dispositifs où les manganites sont intégrés comme composants actifs.

Introduction to Part I

The application of properties of many functional materials require thin film preparation. However, the physical properties of a bulk material as magnetic anisotropy, magnetic interactions as well as structural and electric properties can be highly modified if it is grown as a thin film due to the induced substrate strain or tuning the surface to volume ratio.

This is the first work devoted to manganite oxide films in the Laboratory Louis Néel-CNRS (Grenoble). The objective of the present work has been the study of the growth and the optimisation of manganite films on single crystalline substrates, as well as the study of their magnetic and transport properties with special emphasis on spin dependent transport. This objective implied the development of a new deposition chamber specially adapted for oxide growth (Appendix A:). Consequently, I devoted a considerable amount of efforts in the design and set-up of the new laser ablation chamber that has been entirely “home-made”.

In **Part I,** we firstly give a general description of manganese oxides. Their crystallographic structure, as well as main magnetic and electric properties, relevant for the present work, are described (chapter 1). Secondly, a short introduction to the basis of charge transport in ferromagnets, as well as to the spin dependent transport (magnetoresistance) and their origin, is given (Chapter 2).

The study of the growth of $La_{2/3}Ca_{1/3}MnO_3$ on non matched substrates is undertaken and the effects of granularity as well as the phenomena associated to the Powder magnetoresistance are studied on polycrystalline films and on unconventionally induced grain boundaries (Chapter 3).

The effect of the stress induced by epitaxial growth on slightly mismatched substrates, on the crystallographic, magnetic and transport properties are discussed and analysed (Chapter4).

The originality of the present study is that, while huge efforts have been done for obtaining manganites exhibiting large values of magnetoresistance at room temperature and heterostructured systems as spin tunnel junctions, few groups have worked on the understanding of the spin transport through manganite interfaces. Only recently, some groups began studying the variety of phenomena associated to polycrystalline manganites.

In our opinion, the understanding of the spin transport through grain boundaries or of the effect of strain in manganite films is a fundamental issue before developing devices where manganites are integrated as active components.

Chapitre 1:

Perovskites de Manganèse

1 Manganese perovskites

The manganese perovskites are a large family of oxides with composition $(A^{+3})_{1-x}(B^{+2})_xMnO_3$ where A is usually a rare earth ion and B is an alkaline ion. They exhibit a rich phase diagram under doping and, while the end members (x=0, x=1) are antiferromagnetic insulators, intermediate doping brings the system either FM-metal, charge ordered (CO) insulating, orbitally ordered (OO), paramagnetic (PM)-insulator and more rarely FM-insulator. Huge efforts have been dedicated since 1995 to study these materials but many the essential points for their full understanding remains controversial.

1.1 Introduction

Considering a pure ionic model, in the non doped compound $LaMnO_3$, Mn ion has only the valence +3. The substitution of La^{+3} by divalent ions like Ca^{+2}, Sr^{+2}, Pb^{+2}, Ba^{+2} creates mixed valence: Mn^{+3}/Mn^{+4}.

The phase diagrams of manganese perovskites are extraordinarily complex because the charge, spin and lattice degrees of freedom are strongly coupled. The main competing interactions are the ferromagnetic double exchange (FM-DE), the antiferromagnetic or ferromagnetic superexchange interaction (SE), in addition to the electron-phonon coupling through local Jahn–Teller distortions and the co-operative Jahn-Teller energy (giving orbital ordering due to e_g degeneracy). The strong competition among all these couplings (in most cases being of the same magnitude) is at the origin of many interesting phase transitions when an external parameter like the temperature, a magnetic field, hydrostatic pressure are changed.

1.2 Crystal Structure

From the crystallographic point of view, mixed valence manganites have the perovskite structure (perovskite is the mineral $CaTiO_3$) (Fig. 1-1,Fig. 1-2). The ideal chemical formula for such a crystallisation is ABX_3 , where A is a large cation, B is a smaller cation and X is an anion [6]. The stability of such a crystallographic structure is based on several conditions:

-B site ions must prefer octahedral coordination and should have a charge

-A site ions must be big enough to allow the structure not to collapse into a rhombohedral or lower coordinated B site structure and small enough to optimise the B-X bond length.

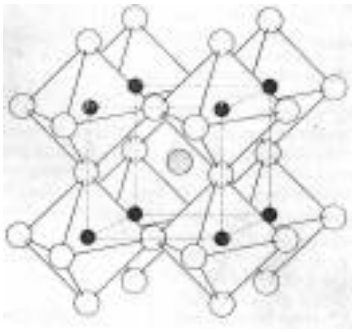

Fig. 1-1 *Perovskite structure centred in the A ion*

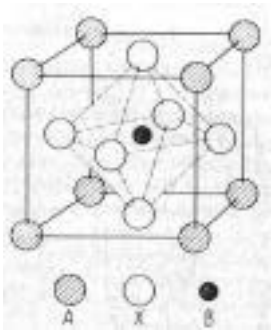

Fig. 1-2 *Perovskite structure centred in the B ion*

The ideal cubic structure in perovskites is rarely found due to the difference in ionic radii of the cations. Goldschmidt studied the stability of the perovskite structure and defined the tolerance factor *t* as $t = \frac{(r_A - r_X)}{\sqrt{2}(r_B + r_X)}$ where r_i are the (empirical) ionic radii. The ideal cubic perovskite has a tolerance factor t=1 and the perovskite structure is stable in a tolerance factor range of $0.75<t<1$(analogous limits are given for the cations radii (r_A>0.90Å and r_B>0.51Å)).

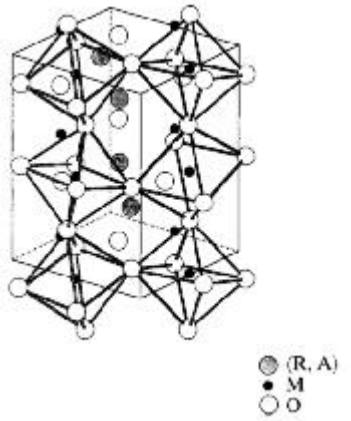

Fig. 1-3 *Buckling of the oxygen octahedra giving rise to orthorhombic structures (Pbnm, $GdFeO_3$ like distortion).*

Perovskite structure has a wide range of stability because it allows deformations of the structure. When *t* is slightly different than 1, there exist a rhombohedral (R-3c) deformation of the structure where the octahedra are tilted around the [111] direction. For lower values of *t*, there appears a buckling of the octahedra around the [110] direction leading to orthorhombic crystal symmetry (Pbnm) (Fig. 1-3).

There is a strong coupling between the structure and the electronic configuration of the mixed valence manganites because Mn^{+3} is a Jahn Teller ion. For certain commensurate values of the doping (x=1/8, 1/3,1/2, 2/3,3/4) in mixed valence manganites, there exist experimental evidences which agree with the existence of a ordered localisation of the charges (Mn^{+3}/Mn^{+4}) which gives rise to structural modulations (in the case of x=1/2 the superlattice seems to be composed by Mn^{+3} and Mn^{+4} ions ordered in the real space as in a chessboard, assuming a pure ionic picture).

There are a few simple crystallographic parameters that can be used to tune the electric and magnetic behaviour of the mixed valence manganites [7-9]:

a) The Mn-O-Mn bonding angle. It can be varied in the range between 180° to ≈156° by A cation substitution or applied pressure. In the case of orthorhombic structures, the bond angle varies continuously with the tolerance factor.

b) The Mn-O bond distance. It controls the overlapping of the Mn 3d and O 2p orbitals

c) The variance ($\sigma^2 = \sum_i y_i r_{A_i}^2 - \langle r_A \rangle^2$) of the cation size at the A sites.

Some of these tuning mechanisms have been explored in the last six years to understand the interactions giving rise to the colossal magnetoresistance.

In the following section, the electronic structure of manganites will be briefly introduced.

1.3 Electronic structure

The spectacular diversity of magnetic and electronic phases in mixed valence manganites is consequence of an interesting evolution of electronic structure through doping. The end members and non-doped compounds of the manganite family $LaMnO_3$ and $CaMnO_3$ are both insulating and antiferromagnetic (AF) but the AF order is different.

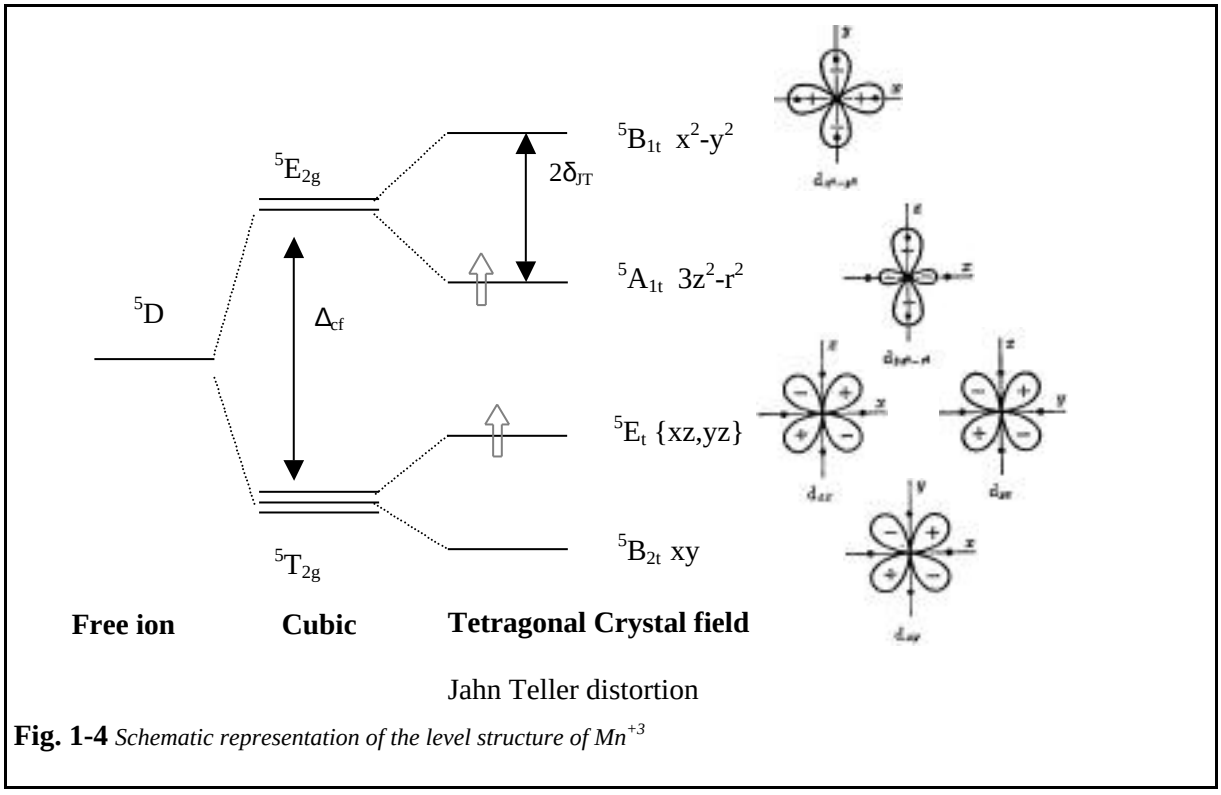

Fig. 1-4 *Schematic representation of the level structure of Mn^{+3}*

In $LaMnO_3$ all the Mn ions have a valence +3 while $CaMnO_3$ is entirely composed by Mn^{+4} ions. $Mn^{+3}(3d^4 4s^0)$ in a cubic crystal field lose the five-fold degeneracy of the *d* states that split into

two fold degenerate *E* and three-fold degenerate T_2 levels. T_2 orbitals go through the directions bisecting the angle between two coordinate axis (xy,xz,yz) while *E* orbitals have lobes pointing the coordinate axis (x^2-y^2, $3z^2$-r^2). As the *E* lobes are directed towards the anions (0^{-2}) the electrostatic energy will increase the energy of the *E* levels compared to that of the T_2 ones. In addition, Mn^{+3} is a Jahn Teller (JT) ion and the Jahn Teller Theorem (1936) predicts that:

> " If the symmetry of the crystal field is so high that the ground state of an ion is predicted to be orbitally degenerated, then it will be energetically preferable for the crystal to distort in such a way that the orbital degeneracy is lifted".

That is the case for Mn^{+3} in a cubic crystal field. The JT tetragonal distortion of the octahedra lifts the degeneracy of the orbitals (Fig. 1-4). JT distortion can be dynamic or static. In the dynamic JT distortion, the system can tunnel between energetically equivalent distortions giving rise to a resonant state. This dynamic JT state is averaged out in crystallographic meures but can be deduced from the high value of the Debye Waller parameters in diffraction measurements [10]. The cooperative static JT distortion gives rise to the ordering of the octahedra in the crystal. Such ordering can change the global symmetry of the system.

Each of the three $^5T_{2g}$ (t_{2g}) orbitals are half occupied with the spins coupled FM giving rise to S=3/2, while the e_g orbitals are empty for Mn^{+4} and half occupied in Mn^{+3}. A strong Hund's coupling ($J_H \approx 2$-3eV), larger than Δc_f, gives rise to a high spin configuration in Mn^{+3}.

In $LaMnO_3$, the crystal field splitting (Δ_{cf}) is about 1.5 eV [11] while the Jahn Teller splitting ($2\delta_{JT}$) is about 1eV.

1.4 Magnetic interactions

In mixed valence manganites, the ions contributing to the magnetism are mainly the Mn. Some long range order on the rare earth (RE) lattice due to the effective field created by the Mn lattice has been experimentally found [12] but it is still a controversial. And RE order due to RE-RE dipolar coupling only takes place at rather low temperatures (≈1K in $PrGaO_3$).

The magnetic interaction between manganese ions is not a direct exchange interaction, it is indirect exchange mediated by the oxygen anions. There exist two mechanisms for indirect coupling in manganites: Superexchange (SE) and Double exchange (DE).

The sign of the SE magnetic coupling depends on the orbitals shared with the anion as set by Goodenough-Kanamori rules. SE gives AF coupling when the Mn orbitals shared with the oxygen anion are both empty, half or full filled but the orbitals involved are the same. On the other hand, the SE can give also FM coupling when the orbitals shared with the oxygen anion are different Mn orbitals.

The FM DE interaction competes with the antiferromagnetic S=3/2-O-S=3/2 superexchange (SE) interaction. In DE mechanism, the electron keeps its spin during the hopping process between Mn^{+3}-O-Mn^{+4} and the effective transfer integral, t_{ij}, can be expressed as $t_{ij} = t_{ij}^{0} \cos\left(\beta_{ij}/2\right)$ where β_{ij} is the angle between the t_{2g} localised moments of neighbouring Mn. Due to the intratomic Hund's coupling the e_g electron has its spin aligned with the localised (t_{2g}) moment of the Mn^{+3}. Hence, hopping probability is maximised when the t_{2g} localised moments between adjacent Mn ions are FM aligned.

Double exchange theory was first sketched by Zenner[13], Anderson [14] and de Gennes[15, 16]. Goodenough and Kanamori worked out the magnetic coupling in oxides extending the SE theory when covalence effects play an important role [17]. SE theory was developed by Anderson[18].

1.5 Magnetic phase diagrams

The first studies of the magnetic transitions and structures of manganite compounds were performed in the fifties [3, 17, 19, 20]. Since then, few new magnetic structures have been reported. Although the magnetic phase diagram is not unambiguously described, the low doped region (x≈0) has been extensively studied and there are certain doping regimes where there exist evidences of phase segregation (Part II)[21-23].

The particular phase diagram of manganites strongly depends on the RE and the divalent cation substitution (Fig. 1-5). We will consider the $La_{1-x}Ca_xMnO_3$ family to describe the magnetic phases.

The undoped compound $LaMnO_3$ has an antiferromagnetic A-type magnetic structure due to the orbital ordering of alternating $d_{3x^2-r^2}$ and $d_{3y^2-r^2}$ orbitals in the *ab* plane. The A-type AF spin arrangement consists in FM *ab* planes coupled AF along the *c* axis (Pbnm setting). Doping with divalent cations (Ca) reduces the number of Mn^{+3} ions and thus weakens the orbital ordering and the Jahn Teller distortion giving rise to FM states for dopings higher than 0.10. This ferromagnetic ground state is stable until dopings of around x~0.5 in the case of $La_{1-x}Ca_xMnO_3$. At x=0.5 doping, the ratio Mn^{+3}/Mn^{+4}=1 and upon cooling the e_g electrons tend to localise at certain Mn sites forming a chessboard structure in the *ab* planes. Alternating sites occupied by e_g electrons present Jahn-Teller deformation producing a structural transition. The x=1/2 charge ordered phase (CO) has been described as displaying the CE type AF magnetic structure[20]. Larger doping levels give rise to a series of AFM and CO states that are studied in detail in chapter 8 on the bismuth based family.

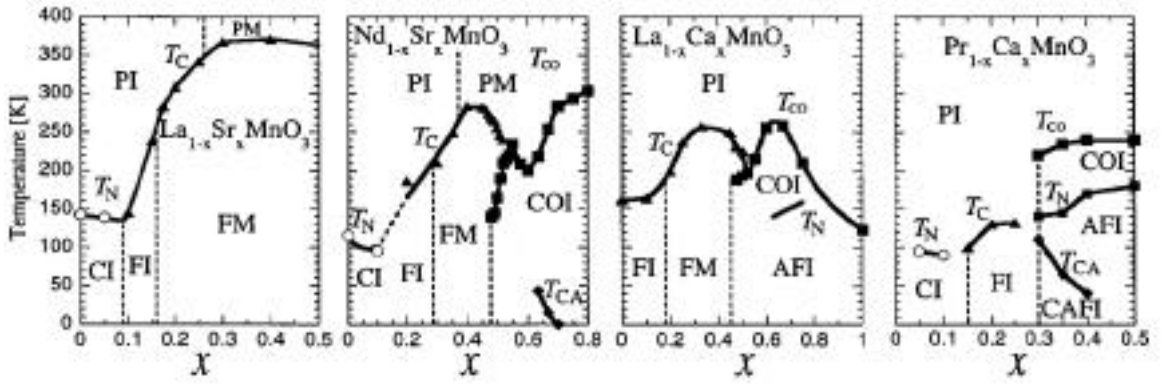

Fig. 1-5 *Magnetic and electrical phase diagrams of four characteristic mixed valence manganese families. T_C is the Curie temperature, T_N is the Neel temperature, PI,PM and CI denote paramagnetic insulator, paramagnetic metal, spin canted insulating phases. FI, FM and AFM denote ferromagnetic insulator, ferromagnetic metal and antiferromagnetic (A type) metal. COI denotes the CE charge ordering insulating state. CAFI denotes the canted antiferromagnetic insulating sate.*

In Part I we will focus on a ferromagnetic and metallic compound (x=0.3) exhibiting the paramagnetic to ferromagnetic (PM-FM) transition. This transition occurs in a particular way. The existence of local lattice distortions due to polarons in the PM phase has been experimentally suggested by X-Ray absorption fine structure [24], small angle scattering and optical experiments [25-27]. This anomalous transition has also been studied by Muon Spin Relaxation and an evidence for a broad distribution of anomalously long and spatially inhomogeneous Mn-ion correlation times near and below T_C has been reported [28]. Electronic Paramagnetic Resonance (EPR) measurements seem to agree in the fact that close to the transition (below 600K for $La_{0.7}Ca_{0.3}MnO_3$ with T_C=270K) the moments consist in cluster of several spins [29]. NMR studies on samples showing the PM-FM transition agreed with the existence of magnetic polarons or ferromagnetic clusters near T_C [30]. Thermal expansion measurements also show expansion anomalies up to temperatures of the order of $\approx 2T_C$. These thermal anomalies are sensitive to the magnetic field (0.1% of magnetostriction [31]) and can be suppressed by an applied magnetic field of around 10T in $La_{0.60}Y_{0.07}Ca_{0.33}MnO_3$.

The $La_{2/3}Ca_{1/3}MnO_3$ compound exhibiting the PM-FM transition has been reported to behave as an isotropic Heisenberg ferromagnet with an exchange coupling constant J=21.8K [32], and a gapless dispersion relation $E=Dq^2$ with a spin wave stiffness of D=170meV Å^2 at low temperature.

Metallic and ferromagnetic manganites were found theoretically from structure band calculations to be half-metals. In the following section, we will describe the half-metallicity.

1.6 Half-Metals

Experimentally, only three transition elements (Fe, Co and Ni) exhibit ferromagnetism at room temperature. Partially filled 3d level is responsible for the magnetism in the ferromagnetic transition metals and the conduction band has a 3*d*-4*s* character.

In the case of FM metallic compounds, the majority spin and minority spin bands are asymmetric and the density of states at the Fermi level is different for both spin directions.

Band structure calculations predicted the existence of special kind of ferromagnetic materials that would have 100% polarised conduction band. These are some semi-Heusler alloys like NiMnSb or PtMnSb [33], some manganites, CrO_2, Fe_3O_4 and the double perovskites Sr_2MnFeO_6. These materials are called half-metallic ferromagnets because they have a metallic density of states in one of the spin channels and a gap in the density of states in the other channel. This is the limit of the asymmetric band configuration.

In the Fig. 1-6 is shown the band structure of the manganese oxide's parents compounds [34]. It is also shown the calculated density of states for the majority and minority spin bands for the FM and metallic compound $La_{2/3}Ca_{1/3}MnO_3$ [35] (Fig. 1-7). When doping $LaMnO_3$ with divalent cations, the $e_g\uparrow$ band crosses the Fermi level, while no available density of states is present for the down majority spin.

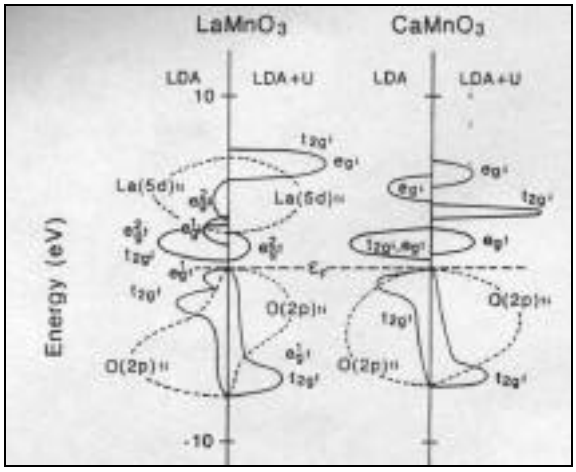

Fig. 1-6 *Density of states of the parents compounds $LaMnO_3$ and $CaMnO_3$ both antiferromagnetic and insulator from [34]*

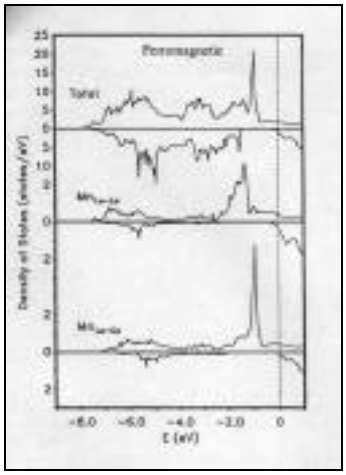

Fig. 1-7 *Density of states for $La_{0.7}Ca_{0.3}MnO_3$ [36]*

In the Fig. 1-8 is shown one of the experimental proofs (controversial for certain authors) of the half metallicity of the $La_{0.7}Sr_{0.3}MnO_3$ compound. It consist in spin resolved photoemission experiments performed on manganites by Park et al.[37]. At 40K there exist a gap of 0.6 eV between

the spin up and spin down bands consistent with the definition of half-metal. At 300K no difference between the spin up and down bands is observed.

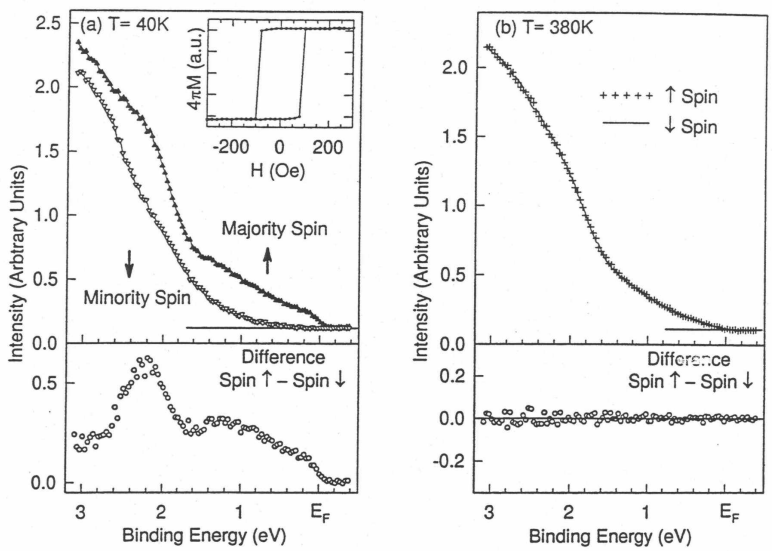

Fig. 1-8 *Spin resolved photoemission experiments performed on $La_{0.7}Sr_{0.3}MnO_3$ film at 40K and 300K by Park et al.*

1.7 Electric Transitions

One of the interesting phenomena in mixed valence manganites is the strong relation between transport and magnetism. This relation can be, in first approximation, understood based on the DE theory even if the DE-only model does not fully explain all the features observed in the ferromagnetic and metallic compounds [38]. In this sense, a strong electron phonon coupling has been experimentally checked by isotopic oxygen substitutions (O^{16}-O^{18}, $\Delta T_C/T_C \approx 10\%$) [39, 40]. Such coupling is evidenced by the existence of bounded states of the charge and spin carriers and the phonons (magnetic polarons) as observed by different techniques in the PM-Insulating state slightly above the M-I transition temperature [41].

The metallic phase in FM manganites is characterised by relatively high residual resistivity compared with usual metals ($\rho_0(La_{0.7}Ca0.3MnO_3$ single crystal)$\approx$ 140μΩcm, ρ_0(Co)=0.16±0.03μΩcm or ρ_0(Fe)=0.36±0.04μΩcm)[42 , 43] and a hopping type transport mechanism. However, the value of the residual resistivity depends highly on the sample preparation and microstructure. The introduction of crystallographic grain boundaries increases the residual resistivity several orders of magnitude. In thin films processing the substrate surface, post-annealing treatments as well as strain can tune the value of ρ_0.

In ferromagnetic and metallic manganites, two important parameters control the kinetic energy of the conduction electrons and determine the metal insulator transition temperature:

a) the band filling (doping)

b) the bandwidth (*w*)

The band filling is changed by cation (ionisation state<+3) substitution at the rare earth site. The bandwidth or electron hopping interaction can be modified in several ways: I) External pressure, II) Internal chemical pressure, II) Ionic size variance at the A site.

The electron bandwidth is related to the integral transfer ($w=2zt_{d\text{-}p\text{-}d}$) because the electron transfer between neighbouring Mn sites is done via the oxygen 2*p* states. In nearly cubic perovskites and in the strong ligand field approximation the *p-d* transfer integral is proportional to $t^0_{pd}\cos(\text{Mn-O-Mn})$, where t^0_{pd} is the transfer integral for a cubic perovskite. Moreover, the $t_{p\text{-}d\text{-}p}$ transfer integral is approximated to the square of the *d-p* transfer integral. Hence, bending the Mn-O-Mn bond angle, produces a reduction of the single electron bandwidth which is proportional to $\cos^2(\text{Mn-O-Mn})$[44].

Hydrostatic pressure on compounds exhibiting the metal-insulator transition has been shown to increase the bandwidth by increasing the overlapping of the Mn-O orbitals ($d_{Mn\text{-}O}$). The widening of the bandwidth gives rise to an increase of the M-I transition temperature [45, 46]. On the other hand, external uniaxial pressure on single crystals has revealed to give rise to anisotropic distortions which tend to localise the carriers and thus narrowing the bandwidth and reducing the M-I transition temperature [47]. In chapter 4, we discuss the effect of epitaxial strain on the electrical transport of ferromagnetic and metallic compound.

It is called internal chemical pressure, the effect of the substitution of the rare earth cation by another rare earth of different radius for a fixed doping. Smaller rare earth, give rise to more distorted perovskite structures while substitution by larger ion size rare earths often results in an increase of the M-I transition temperature [7, 48].

In compounds with equal mean A site ion radius, the effect of the ion size variance is to localise the carriers and to decrease the M-I transition temperature [9]. This effect is originated by the random potentials originated in the material due to large differences on the ion size.

In the lattice-polaron DE model, the crossover from metallic to insulating behaviour is controlled by the ratio:

$$\lambda = \frac{E_B}{E_{kin}} \qquad \textbf{Eq. 1-1}$$

E_B is the polaron binding energy and E_{kin} is the kinetic energy of the carriers. For $\lambda<1$ the system tends to be in the metallic state while for $\lambda>1$ the insulating state is more favourable. In order

to obtain the doping dependence of E_{kin} some authors introduced the effect of orbital fluctuations and orbital polarons [49].

In Fig. 1-5 are shown the electrical transitions exhibited by different manganite compounds as a function of the band filling (*x*), and as a function of the lattice distortion (distortion (LaSr)>(NdSr)>(LaCa)>(PrCa)). There exist a tight relation between the magnetic and electrical transitions. However, even if FM and insulating phases are sometimes observed, the insulating state is mainly associated to AF or PM states while FM is associated with metallic states. It can also be observed that the range in doping level were the FM metallic state is stabilised is narrow. As CMR effects are associated to the FM-PM transitions, CMR can only be observed in narrow regions of manganites phase diagrams as for example x≈0.3. In chapter 8 is shown that MR can be also found in a narrow range in the highly hole doped region of the phase diagram.

Chapitre 2:

Propriétés de transport dans les matériaux ferromagnétiques

2 Transport properties in ferromagnets

2.1 Introduction to the electrical transport in oxides

Oxides exhibit a large diversity of transport behaviours. They can be found usually insulating, but some metallic (CrO_2, Fe_3O_4, V_2O_3, VO_2) , semiconducting (EuO) or even superconducting oxides (YBCO).

The electrical properties of conducting oxides are mainly determined by their ionic character. In addition, in transition metal oxides, the "conduction band" is mainly formed by oxygen *2p* and transition metal *d* orbitals while in metals the *s* orbitals play an important role. Thus, while in pure metals the potentials due to defects are screened within a short distance, in conducting oxides, the quasiperiodicity of the potentials (created mainly by the static distribution of the ions) tends to localise the electrons [50], giving rise to shorter mean free path for the conduction electrons. For that reason, conducting oxides are highly sensitive to external parameters as temperature, pressure, doping… In this sense, some oxides exhibit a metal insulator (M-I) transition at certain temperature, or change their ground state under doping (Nb doping on $SrTiO_3$ gives rise to insulating to superconducting transition).

From the transport point of view, the principal units of transition element oxides are the MO_6 octahedron or the MO_4 tetrahedron where the metal-*d*-orbitals overlap the *2p* oxygen orbitals forming extended orbitals.

For certain doping levels of manganese oxides magnetoresistance appears and it has been called Colossal Magnetoresistance. In the following section, we will introduce the different mechanisms giving rise to magnetoresistance and it will be straightforward to understand why the magnetoresistance in manganites is called Colossal.

2.2 Mechanisms for magnetoresistance

Magnetoresistance (MR) is the change in resistivity under the application of an external magnetic field (H).

In the absence of a magnetic field the conductivity (or resistivity) tensor is symmetrical ($\rho_{ij}=\rho_{ji}$) and can be diagonalised. When a magnetic field is applied ρ_{ij} is not, in general, symmetrical. However, frequently the coupling between longitudinal (J||H) and transverse (J H) effects is negligible. That means that if there is an applied field in the *z* direction the resistivity tensor for a cubic system becomes:

$$[\rho_{ij}] = \begin{bmatrix} \rho(B) & -\rho_H(B) & 0 \\ \rho_H(B) & \rho(B) & 0 \\ 0 & 0 & \rho_{II}(B) \end{bmatrix} \qquad \textbf{Eq. 2-1}$$

where means resistivity for J perpendicular to M. ρ_{ij} are function of the induction (**B**), which depends on the applied magnetic field (H), the magnetisation of the sample (M), and the demagnetising factor, D : $B = \mu_0 (H + M(1-D))$). Off diagonal elements are related to Hall Effect.

The magnetoresistance is usually expressed as:

$$MR(\%) = \frac{\rho(H) - \rho(0)}{\rho(0)} \quad 100 \qquad \textbf{Eq. 2-2}$$

In the following sections a brief description of the different mechanisms for magnetoresistance are presented in order to understand the difference between the Colossal Magnetoresistance (CMR) present in some manganite compounds and the other kinds of magnetoresistance.

2.2.1 Cyclotron Magnetoresistance

The effect of a magnetic field on the conduction electron in a non magnetic material results from several processes. On the one hand, under a magnetic field and from a classical point of view, a conduction electron travelling in a direction non parallel to the magnetic field direction will tend to bend its trajectory giving rise to a precession with a cyclotron frequency $\omega_c = qB/2m^*$ (cyclotron effect). In this case, the effect of the magnetic field is to increase the resistivity and the MR varies as B^2 up to $\omega_c\tau \approx 1$ where τ is the mean free path of carrier. This intrinsic MR is called cyclotron and has a value of around 1% in 1T.

In manganites, cyclotron magnetoresistance is very small and $\omega_c\tau \approx 2\ 10^{-4}$ at 1T.

2.2.2 Anisotropic magnetoresistance

The anisotropic magnetoresistance (AMR) is the change in resistance when the electrical current is parallel or perpendicular to the internal magnetisation (Fig. 2-1). It is an intrinsic effect appearing in certain FM materials. Attention has to be paid to magnetocrystalline anisotropy which can prevent the magnetisation to follow the applied field direction.

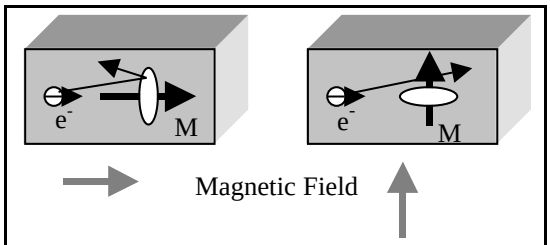

Fig. 2-1 *Schematic representation of the AMR origin*

The AMR is defined as:

$$AMR(\%) = \frac{\rho_{II} - \rho}{\frac{1}{3}\rho_{II} + \frac{2}{3}\rho} \qquad \textbf{Eq. 2-3}$$

AMR can have either signs and its amplitude is ≈1%. It can reach 3% as in the case of alloys of Ni-Co or 2% for Ni-Fe alloys (Permalloy). Unlike CMR it is saturated when the magnetisation is saturated.

AMR in Manganites

In strontium based manganites (x=33%) deposited on $SrTiO_3$ substrates, –0.2% of AMR is obtained at low temperatures. A value of 2% is reached at temperatures close to T_C as reported by Ziese et al. [51-54]. In Fig. 2-2 it is displayed the data extracted from Ziese's article showing in dashed lines the magnetoresistance with the current in the plane of the film and perpendicular to the field direction. In continuous line the magnetoresistance with the current and applied field parallel. Transverse resistivity is larger than longitudinal which leads to a negative AMR. In order not to take into account other effects than purely AMR and not CMR effects, AMR value is determined in a field of 0.03T in which the sample is magnetically fully saturated.

A striking feature of the AMR observed in manganite film is that it peaks close to T_C and it decreases when reducing temperature in contrast to FM alloys where AMR scales with the magnetisation square of the sample. On the other hand, the AMR in manganites decreases with the applied field, which contrast with the slight increase of the AMR with the applied magnetic field in FM alloys. Therefore, conventional AMR theory does not apply in thin manganite films. O'Donnell et al. proposed that AMR in manganite thin films is due to a local, spin-orbit induced, orbital deformation which change the orbital overlap between neighbouring ions when the magnetisation is rotated due to the fact that the lattice parameter of the films is locked by the substrate. However, a qualitative understanding of the AMR in manganites has not been achieved.

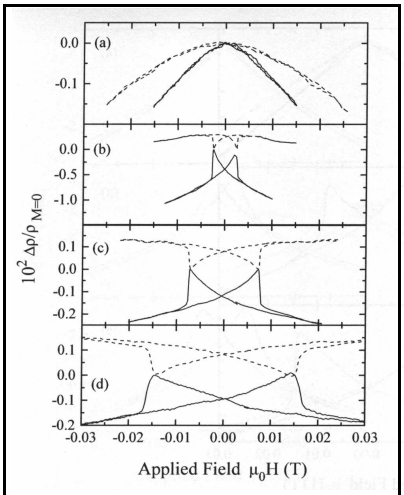

Fig. 2-2 *Figure extracted from Ziese et al. article displaying the AMR in a LCMO film on STO at a) 285K, b) 264K, c) 201K and d) 96K. Solid lines in the figures consist in longitudinal configuration while dashed lines are transverse measurements.*

2.2.3 Giant magnetoresistance (GMR)

Giant magnetoresistance is a very general term but has been assigned to the case of the resistance change when, in non homogeneous systems with FM zones magnetically decoupled by conducting zones. The relative orientation of the magnetisation in the layers goes from AF to F under the application of an external magnetic field (Fig. 2-3). In contrast with the AMR, the GMR is an extrinsic process. GMR values can be larger than AMR.

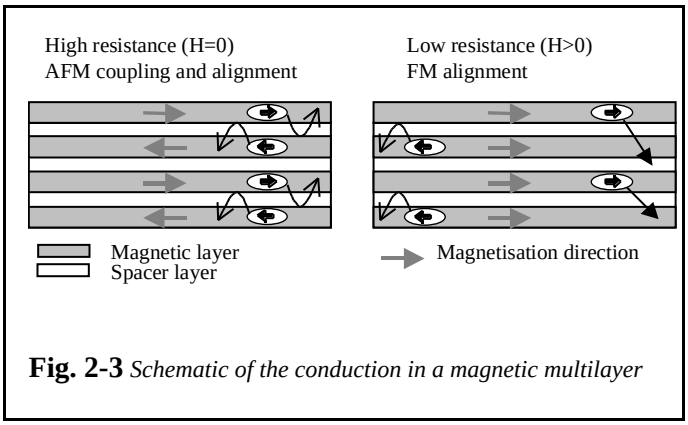

Fig. 2-3 *Schematic of the conduction in a magnetic multilayer*

The first observations of GMR were in 1988, in heterostructures of Fe/Cr(001) deposited by MBE [55]. In such system they reached 50% of GMR[1] at 4.2K and 12% at RT for fields around 20kOe. In 1990 Parkin et al. [56] evidenced the oscillations in the GMR as a function of the non-magnetic layer thickness in heterostructures deposited by sputtering of TM/Cr (TM=transition metal). These oscillations reflect the coupling oscillations and their damping with the increase of the spacer thickness is due to the nature of the RKKY interaction. The dependence of the GMR with the magnetic layer thickness suggests also an important bulk contribution in addition to the interfaces contribution.

The origin of such MR comes from the spin-dependent diffusion at the interfaces and the effect of a periodic potential connected to the superstructure.

The characteristic lengths which characterise the GMR structures depends on the geometry. In the CIP (Current In Plane) arrangement, the characteristic length is the mean free path of the carriers, hence, the thickness of the non magnetic layer should be less than the mean free path for the conduction electron. In the CPP (Current Perpendicular to the Plane) arrangement, the characteristic length is the spin diffusion length of the conduction electron thus determining the thickness of the non magnetic layer. These lengths correspond typically to 100Å and 1000Å respectively.

In addition, in GMR systems, the resistance depends on the angle between magnetisation direction in adjacent magnetic layers and varies as cos θ.

[1] GMR is usually defined by the optimistic formula: GMR= $\Delta R/R(H)$ and $\approx \Delta R/R(0)$ when MR is small

The CPP geometry gives higher values of GMR because there is no shunting current through normal metals and the conduction electrons are forced to go through all the interfaces increasing the scattering effects at the interfaces and also the value of GMR.

For applications, an improvement of GMR structures has been the development of spin valves. These structures are more complex than previous ones. There is a difference in the nature of the two magnetic layers: one is a hard ferromagnet (hence high H_C or pinned layer) while the other is a soft ferromagnet with a magnetisation that can be rotated under the application of very low fields. Systems as Co/Cu/NiFe[57] exhibit 20% of magnetoresistance at RT under an applied field of 10Oe. That means 2%/ Oe in sensibility.

2.2.4 Tunneling magnetoresistance (TMR)

Tunneling magnetoresistance (TMR) appears in heterostructured systems formed by ferromagnetic and metallic electrodes separated by an insulator spacer. The spacer uncouples magnetically the layers and breaks the metallic conduction channel, so only tunneling of carriers is possible. TMR appears due to the carriers polarisation in the metallic ferromagnets and it exploits the asymmetry in the density of states of the majority and minority energy bands at E_F .

Spin polarised tunneling (SPT) was discovered in 1970 by Tedrow and Meservey [58, 59]. Tedrow and Meservey used a superconducting electrode (Al), and measured a spin polarisation in FM metals at low temperature. This measurements revealed that spin direction is conserved in tunneling processes (see [60] for an extensive review about SPT).

Tunneling probability depends on the relative orientation of the magnetisation in the FM layers. When using symmetrical electrodes, in the parallel configuration, there is a maximum match between the number of the occupied states in one electrode and the available states in the other and the tunneling resistance is minimum. In the antiparallel configuration, the tunneling is between majority states in one electrode and minority states in the other so the resistance is higher.

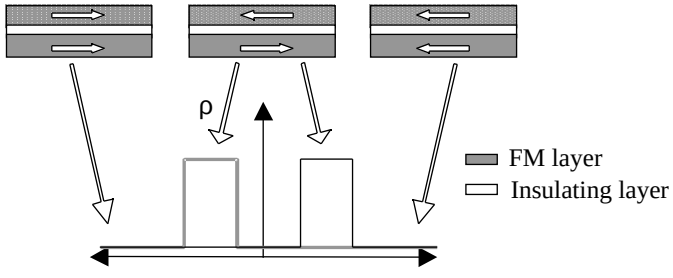

Fig. 2-4 *Schematic representation of a tunnel junction*

The first experiments on ferromagnet/insulator/ferromagnet tunnel junctions were performed on Fe/Ge/Co trilayers [61]. The difference in coercive field permitted to make the magnetisations of the films to be parallel, or antiparallel (Fig. 2-4).

Julliere described the TMR when switching the trilayer from the parallel configuration of the electrodes (described by its resistivity ρ_p) to the antiparallel configuration (ρ_{ap}) as a function of the electrodes spin polarisation (*P,P'*):

$$\frac{\Delta\rho}{\rho_{ap}} = \frac{\rho_{ap} - \rho_p}{\rho_{ap}} = \frac{2PP'}{1+PP'} \qquad \textbf{Eq. 2-4}$$

Experimental values of the spin polarisation *P* of metallic ferromagnets has been reported by performing tunneling experiments with superconducting electrode as spin detector [62] or by Andreev reflection measurements [63]. However the obtained polarisation values for a certain material using one or the other techniques are different (Fig. 2-5) and are unable to give the thermal evolution of the polarisation because such techniques can only be used at very low temperatures. Consequently, there is a renewed interest on these phenomena and on the definition and identification of the measured spin polarisation [64].

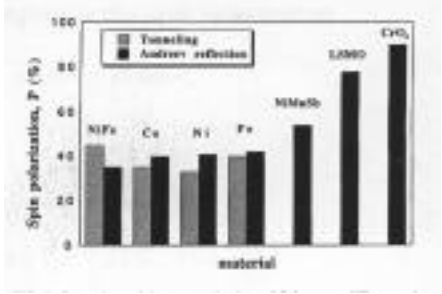

Fig. 2-5 *Experimental values of the spin polarisation obtained from tunneling and from Andreev reflection experiments*

In the first reported trilayers using Co, Fe or even manganites, the experimental MR was lower than the one calculated from the obtained polarisations of Co, Fe or $La_{0.7}Sr_{0.3}MnO_3$ from tunneling in a superconductor/insulator/metal measurements [65] or Andreev reflection [63]: 33%for Ni, 45% Co, 45% for Fe, 48% $Ni_{80}Fe_{20}$ and 80% for $La_{0.7}Sr_{0.3}MnO_3$ as shown in Fig. 2-5. In addition, it has been experimentally demonstrated that the deduced spin polarisation value obtained from tunneling experiments depends strongly on the nature of the insulator used thus suggesting that the polarisation of the tunneling carriers given by Julliere's formula can be different from the spin polarisation of the conduction band in the metal electrode [66]. This difference is attributed to the modification of the band structure at the metal/insulator interface. As tunneling electrons come mostly from the first layers of the metal close to the interface, such change in the band structure will modify the polarisation of the electrons at the Fermi level. Calculated electronic structure of junctions Fe/Ge/Fe[67] show some changes in the minority and majority density of states at the Fermi level for the metallic planes adjacent to the Ge layer. In this system, the minority density of states near the Fermi level is enhanced.

The *dc* bias dependence of TMR can be attributed to the influence of the applied electric field on the barrier. Increasing the dc bias increases the conductance and decreases the value of TMR. The important factors that influence the value of TMR are the barrier quality, the FM/I cleanliness, and the well-defined and separated values of H_C for the two electrodes. Values of TMR of around 20.2% at RT and 27.1% at 77K are reported for $Co/Al_2O_3/NI_{80}Fe_{20}$ [68].

Measuring the I(V) characteristics in tunnel junctions, some parameters as the barrier height or thickness, can be obtained as deduced by Simmons [69]. He established that tunneling current density through the barrier is:

$$J = J_0 \left\{ \bar{\varphi} \exp(-A\bar{\varphi}^{1/2}) - (\bar{\varphi} + eV) \exp\left[-A(\bar{\varphi} + eV)^{\frac{1}{2}}\right] \right\}; \qquad J_0 = \frac{e}{2\pi h \Delta s} \qquad \textbf{Eq. 2-5}$$

where :

$$A = (4\pi \Delta s / h)(2m)^{1/2} \qquad \textbf{Eq. 2-6}$$

ϕ is the mean barrier energy height

V is the voltage across the junction

Δs is the barrier thickness as shown in Fig. 2-6.

In this approach to the tunneling phenomena, there is no magnetism included. General equations independent of the barrier's shape are obtained as well as analytical equations for the current density for low and high voltage limits.

Helman and Abeles [70] deduced a model to explain the spin-polarised tunneling between FM metallic grains embedded in an insulating matrix. In their model, the granular system is represented by a conductance network with metallic particles connected by weak links. The thermal dependence of

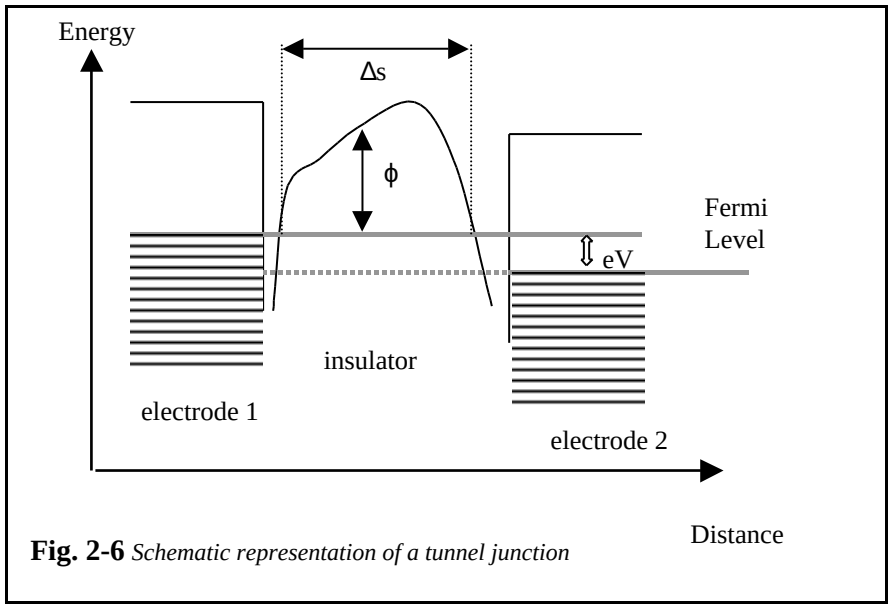

Fig. 2-6 *Schematic representation of a tunnel junction*

the resistivity of the system being:

$$\rho \quad \exp\left(\frac{\Delta}{k_B T}\right)^{\frac{1}{2}} \qquad \textbf{Eq. 2-7}$$

where Δ is related to the electrostatic charging energy $E_c=e^2/2C$, needed to generate a positive and negatively charged grains when the electron tunnel from one grain to the other. When including the magnetism in the above model, the authors suggested the addition of an extra energy term which takes into account the exchange energy which arises when the magnetic moments of the grains are not parallel and the electron conserves its spin direction when tunneling. The authors deduced that under the application of a magnetic field the magnetoresistance of the ferromagnetically coupled grains could be expressed as:

$$\frac{\Delta\rho}{\rho(H)} = -\left(\frac{JP}{4k_B T}\right)\left[m^2(H,T) - m^2(0,T)\right] \qquad \textbf{Eq. 2-8}$$

where J is the exchange constant, *P* is the polarisation of the conduction electrons and *m* is the magnetisation normalised to its saturation value.

Compared to the GMR, TMR systems work always in CPP configuration, give higher values of the junction resistances and the voltage signals involved are of the order of some tenths of Volt giving sometimes rise to the breakdown of the dielectric layer.

TMR in Manganite based Tunnel Junctions

In manganites, the tunneling carriers have a *d* character. In addition, due to the half metallicity of FM and metallic compounds, no current is expected in the antiparallel configuration in tunnel junctions (TJ) due to the absence of available states for the minority spin band. The first fully manganite based TJ was reported in 1996 [72] [73]. It was composed by two epitaxial $La_{0.7}Sr_{0.3}MnO_3$ electrodes separated by an insulating $SrTiO_3$ thin film in the former paper. The reported magnetoresistance ΔR/R is of about 83% and the polarisation deduced is of about 54% at 4.2K. The TMR(ΔR/R) vanishes around 200K. This temperature is smaller than T_C, and suggests that there are spin flip excitation like spin waves at the interfaces or there exists a loss of conduction band spin polarisation upon warming. Other authors [74, 75] have reported higher values for ΔR/R and thus higher values for P of about 65% and 83% which is in better agreement with the theoretically predicted half metallicity of these manganese oxides.

Powder Magnetoresistance (PMR) in manganites

Powder magnetoresistance [76] or intergrain magnetoresistance is a kind of tunneling magnetoresistance. It is an extrinsic magnetoresistance that appears when the conduction band is spin polarised and transport between the grains is possible in compacted powders, granular films or in

artificially fabricated grain boundaries on bicrystal substrates. No exchange coupling between the grains is required.

The name PMR takes into account several phenomena related to the granular character.

The first evidence of such behaviour in manganites was reported by Hwang et al [71]. In this article, no differences on magnetisation measurements or X rays diffraction patterns were detected, and big differences on transport measurements were evidenced between different polycrystalline samples that were annealed at different temperatures and a single crystal (Fig. 2-7). Some theoretical expressions that account for this kind of MR are reported in [77] and in [78].

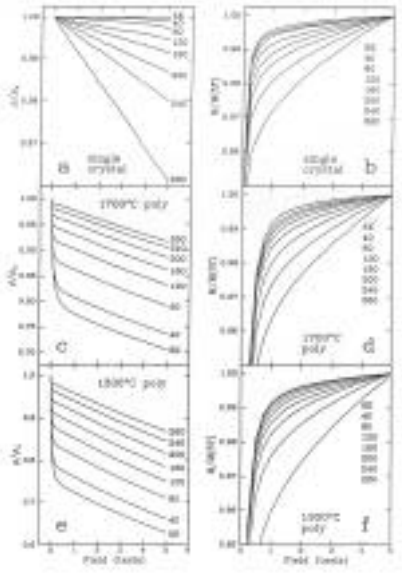

Fig. 2-7 *First evidence of PMR in manganites displaying the differences in resistivity and magnetisation measurements between different polycrystalline samples that have been annealed at different temperatures and a single crystal [71].*

2.2.5 Colossal Magnetoresistance in Manganites

It is called colossal magnetoresistance (CMR) the intrinsic MR present in certain mixed valence manganese oxides (and EuO) which can be as high as 100% and which takes place around the metal insulator transition that occurs close to T_C.

The CMR is usually defined as:

$$\%CMR = \frac{R(0) - R(H)}{R(0)} \quad 100 \qquad \textbf{Eq. 2-9}$$

In Fig. 2-8 is displayed the spontaneous magnetisation as well as the resistivity measured at 0T and 5T for one of our films of $La_{2/3}Ca_{1/3}MnO_3$ (LCMO), about 90 nm thick, grown on $SrTiO_3$ (001) substrate.

The difference between the GMR and CMR is that while the former is an extrinsic effect that exist for temperatures below T_C, the latter is an intrinsic effect, it exists only at the metal-insulator transition temperature close T_C and it is highly reduced in the saturated FM state of the sample. In addition, CMR has shown to be higher as lower is the M-I transition temperature (and T_C) evidencing the intrinsic character of CMR.

The first study on this mixed valence manganites was done by Von Santen and Jonker [2] which published resistivity measurements on the family of compounds $(La_{1-x}A_x)MnO_3$ (A= Ba, Ca, Sr). However, the renewed interest in these materials appeared due to the large magnetoresistance observed at T_C [4].

The CMR is highly related to the fact that the conduction carriers are at the same time responsible of the magnetic coupling.

The optimum doping for achieving the maximum of CMR in the $La_{1-x}(B)_xMnO_3$ family of compounds has been reported to be x=1/3 (B=Ca,Ba,Sr,Pb). High MR has been also observed in higher doping levels as is reported in chapter 8.

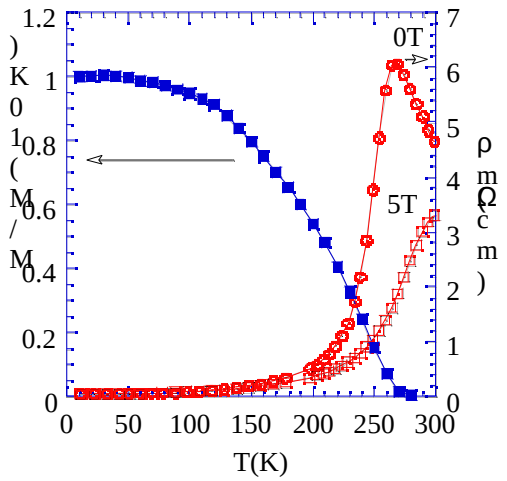

Fig. 2-8 *Spontaneous magnetisation and resistivity at 0T and 5T measurements on a 90nm film of LCMO on $SrTiO_3$ substrate*